



Cite this: *Sustainable Food Technol.*, 2025, 3, 2337

## Microencapsulation of red palm oil with soy protein concentrate–carrageenan conjugates for compound dark chocolate applications

Haida Setyani,<sup>a</sup> Arima Diah Setiowati,  \*<sup>a</sup> Sri Rahayoe,<sup>b</sup> Chusnul Hidayat<sup>a</sup> and Arifin Dwi Saputro<sup>b</sup>

Red palm oil (RPO) is a rich source of carotenoids but is susceptible to degradation and possesses a distinct palm-like odor and taste that may affect the sensory quality of food products. Microencapsulation is considered a potential approach to address these challenges. This study aimed to minimize the aftertaste of RPO through the characterization and formulation of the microencapsulation process. Soy Protein Concentrate (SPC) and carrageenan (CG) were conjugated at various ratios, with the optimal ratio being 3:1, which demonstrated improved emulsifying properties, a higher degree of glycation (DG), and greater formation of Maillard reaction products. The resulting microcapsules exhibited a high encapsulation efficiency of up to 82.27% at an oil-to-wall material ratio of 1:3, along with good color retention and *in situ* absorption, as indicated by 82% carotenoid absorption in an *in situ* intestinal study. The addition of RPO microcapsules to dark chocolate bars did not affect the texture, melting point, morphology, and sensory attributes. However, it had a significant effect ( $p < 0.05$ ) on color and rheology parameters. Overall, the encapsulation of RPO using the SPC–CG conjugate as the wall material effectively masked the inherent palm-like taste and odor of the oil when incorporated into the chocolate product, making them undetectable to panelists. These findings support the application of protein–polysaccharide conjugates as a wall material for encapsulating bioactive compounds in functional food products.

Received 17th June 2025

Accepted 9th September 2025

DOI: 10.1039/d5fb00278h

rsc.li/susfoodtech

### Sustainability spotlight

This study promotes sustainable food innovation by valorizing red palm oil, a carotenoid-rich yet underutilized resource, through microencapsulation with soy protein concentrate and carrageenan, both renewable, plant-based ingredients. The approach enhances RPO's functionality as pro-vitamin A and antioxidant compounds and its sensory acceptability in chocolate applications, supporting reduced reliance on synthetic additives and encouraging the integration of natural, bioactive compounds into sustainable food systems.

## 1 Introduction

Red Palm Oil (RPO) is a natural oil obtained from crude palm oil with saturated fatty acid content ranging from 49.69 to 54.40%.<sup>1</sup> It consists of fatty acids, triacylglycerol, macronutrients such as vitamin A in the form of carotenoids, vitamin E (tocopherols), sterols and squalene. RPO is rich in natural carotenoids (600–1000 ppm), which contain 65%  $\beta$ -carotene, 33%  $\alpha$ -carotene, and 2% other types of carotenoids such as  $\gamma$ -carotene and lycopene.<sup>2–5</sup> However, carotenoids in RPO are prone to oxidation

and degradation when exposed to high temperature, UV light, and oxygen.<sup>6,7</sup> The challenges of fortification with RPO-derived carotenoids include its unfavorable color, taste and odor, as well as low stability.<sup>8</sup>

Microencapsulation technology has been widely applied in food products and has been shown to improve product stability, reduce the degradation of bioactive compounds, extend shelf life, and mask unwanted flavors or odors.<sup>9–12</sup> The microencapsulation process of algae oil produced smaller oil particles, which enhanced the emulsion stability of the product.<sup>13</sup> Furthermore, microencapsulation in fenugreek oil effectively masked the bitter taste and showed a good perspective of oxidative stability over time in fish oil.<sup>14,15</sup> Therefore, encapsulation technology serves as a potential solution to prevent the degradation of RPO. Spray drying is a relatively low-cost method that can be easily scaled up, making it suitable for large-scale productions of micro particles with the desired quality,

<sup>a</sup>Department of Food and Agricultural Products Technology, Faculty of Agricultural Technology, Universitas Gadjah Mada, Jl. Flora No. 1, Bulaksumur, Yogyakarta 55281, Indonesia. E-mail: arima.diah.s@ugm.ac.id

<sup>b</sup>Department of Agricultural and Biosystem Engineering, Faculty of Agricultural Technology, Universitas Gadjah Mada, Jl. Flora No. 1, Bulaksumur, Yogyakarta 55281, Indonesia



particularly in the food and pharmaceutical industries.<sup>16</sup> The spray-drying technique was more effective in maintaining the color stability of microcapsules during 30 days of storage than using the freeze-drying technique.<sup>17</sup>

A critical step in encapsulation is selecting an appropriate wall material. Protein–polysaccharide conjugates are a potential wall material for encapsulation of bioactive materials. This type of conjugate is obtained through the Maillard reaction. Conjugates are obtained through the interaction between the amino group of the protein and the free carbonyl group of the polysaccharide, which forms covalent bonds, resulting in a stronger bond in the wall material.<sup>18</sup> Covalent conjugates are not responsive to pH and ionic strength,<sup>19</sup> making them a robust wall material. The Maillard reaction promotes the formation of large molecules. These molecules consist of hydrophobic fractions derived from partial protein folding and hydrophilic fractions from carbohydrates. This structural alteration enhances the technological properties of the protein.<sup>20</sup> The Maillard reaction is generally regarded as a safe and efficient method to improve the functional properties of proteins, such as emulsification and solubility.<sup>21</sup> Conjugates have amphiphilic properties due to protein groups that are capable of attaching to the oil–water interface layer, while the polysaccharide groups form a thick steric layer that prevents flocculation and coalescence.<sup>22,23</sup>

Soy Protein Concentrate (SPC) has good solubility, adsorbs at the oil and water interface, and exhibits good emulsifying ability,<sup>24,25</sup> making it a good candidate as a wall material. In addition, soy protein is one of the most studied plant proteins in Maillard modification techniques and is considered the most relevant plant food to the formation of Maillard conjugates.<sup>26</sup> In contrast, carrageenan has a stable ability to transmit bioactive compound components.<sup>27</sup> Protein-based emulsion systems have inherent limitations, as their stability is highly dependent on environmental conditions such as pH and ionic strength, which may disrupt the overall emulsion stability.<sup>28</sup> Single-component carrageenan is less effective in stabilizing emulsions, as it tends to result in greater fat droplet aggregation and reduced stability compared to blends with other gums.<sup>29</sup> Consequently, encapsulating wall materials composed of a single constituent often lack the desired functional properties.<sup>30</sup> While many studies focused on enhancing the functional characteristics of proteins through the Maillard reaction using various polysaccharides, limited studies have been performed to evaluate the application of SPI conjugated with carrageenan to encapsulate bioactive compounds.

Previous research on carotenoid encapsulation has focused on improving techniques for efficiently trapping and protecting bioactive compounds. While it is an important aspect, the compatibility of the encapsulated material for food application is equally important. Yogurt enriched with carotene microcapsules showed higher antioxidant activity and contained 16% of the daily requirement of carotene.<sup>31</sup> However, the application of fortified carotene microcapsules in confectionary products, especially chocolates, remains insufficiently explored. Chocolate is a product that presents significant potential as a medium for incorporating RPO microcapsules. With its high sugar and

fat content, the incorporation of RPO microcapsules can improve the nutritional profile of chocolate bars. It was reported that fortification of fish oil, chia seed oil, wheat bran oil, moringa oleifera extract, and phenolic extra microcapsules into chocolate products influenced the texture, viscosity, shelf life, and sensory properties of chocolate.<sup>32–35</sup> However, based on the author's literature study, there is no information regarding the incorporation of RPO microcapsules into chocolate bars. The incorporation of RPO into chocolate products aims to enrich them with carotenoids, thereby enhancing their nutritional profile and potential functional health benefits. The direct incorporation of RPO into chocolate bars may reduce product quality due to potential incompatibility between cocoa butter and RPO and the low stability of carotene. Therefore, micro-encapsulation of RPO is expected to prevent this issue, while masking the undesirable flavor and aroma of RPO, and producing chocolate enriched with carotene.

Therefore, this study aimed to investigate the encapsulation of RPO using SPC–carrageenan conjugates and evaluate its incorporation into a chocolate bar (compound) based on the characteristics of chocolate bars, including texture, viscosity, color, melting point, *in situ* absorption of carotenoids, and sensory evaluation. This study included approaches to produce SPC–carrageenan conjugates as wall materials and microcapsules with high encapsulation efficiency.

## 2 Experimental section

### 2.1 Materials

This study used soy protein concentrate (SPC) with 72% protein content. Carrageenan powder was obtained from Indogum, Jakarta, Indonesia. Red palm oil was purchased from a local market. Sodium Dodecyl Sulfate (SDS), Na-phosphate, Na-carbonate anhydrous, and NaOH were obtained from Merck KGaA (Darmstadt, Germany). HCl was obtained from Mallinckrodt (Staines-upon-Thames, UK). Collata chocolate compound was obtained from PT Gandum Mas Kencana.

### 2.2 Preparation of SPC and carrageenan conjugates

Soy protein concentrate (SPC) and carrageenan (CG) conjugates were formed using the method developed by Kusumastuti *et al.*<sup>36</sup> with slight modifications. The SPC–CG conjugates were prepared first by making SPC and carrageenan solutions. The SPC and carrageenan were mixed at various ratios (1 : 3, 1 : 2, 1 : 1, 2 : 1, and 3 : 1), and then dissolved using deionized water to reach 5% (w/w) total hydrocolloid concentration. The mixture was stirred using a hot plate stirrer at 750 rpm and 40 °C. The pH of the SPC–CG solution was adjusted to 7 using HCl 1 M and NaOH 1 M. The mixture was then dried (Wirastar FDH-8, WIRATECH Group, Indonesia) at 50 °C for 5 hours, as determined by preliminary trials (data not shown). At 5 h, the material was fully dried without visible browning, whereas heating for 6 h resulted in a light-brown discoloration, suggesting the onset of advanced Maillard reaction products. The choice of pH 7.0 allowed better control over the reaction, as the Maillard reaction proceeds more slowly and predictably under



neutral conditions compared with alkaline media.<sup>37</sup> The obtained dried conjugates were ground, sieved, and stored in a refrigerator for subsequent analysis. For comparison, a simple mix SPC–CG was prepared by simply mixing SPC and CG without heat treatment. A simple mix of SPC–CG was prepared at the SPC : CG ratio that exhibited the best properties.

### 2.2.1 Measurement of melanoidin and Amadori products.

Browning intensity and intermediate products were measured as described by Kusumastuti *et al.*<sup>36</sup> A solution of the SPC–CG conjugate at a concentration of 1 mg ml<sup>-1</sup> was prepared by dissolving it in deionized water. The browning intensity and the concentration of intermediate compounds were measured using a UV-Vis spectrophotometer (UV-1800, Shimadzu, Kyoto, Japan) at wavelengths of 304 nm and 420 nm for Amadori compounds and melanoidin.

**2.2.2 Determination of glycation degree (DG).** The degree of glycation (DG) was determined using the phthalaldehyde (OPA) method, following the previous method.<sup>38</sup> The OPA reagent was prepared freshly by mixing 40 mg OPA, dissolved in 2 ml of methanol, with 50 ml of 0.1 M borax buffer (pH 9.7), 5 ml of SDS solution (20% w/w), and 0.2 ml of β-mercaptoethanol. The mixture was then diluted to a total volume of 100 ml. For the analysis, 4 ml of reagent OPA was mixed with 200 μl of the conjugate solution (5 mg ml<sup>-1</sup>). The mixture was incubated at 35 °C for 2 min, and the absorbance was measured at 340 nm using a UV-Vis spectrometer (UV-1800, Shimadzu, Kyoto, Japan). A standard curve was established using 0–2 mM L-lysine standard solutions to determine the concentration of free amino groups. The degree of glycation was calculated using eqn (1):

$$DG (\%) = \frac{A_0 - A_t}{A_0} \times 100\% \quad (1)$$

where  $A_0$  represents the free amino group content of unheated SPC and CG mixture, and  $A_t$  represents the free amino group content of SPC and CG conjugates.

**2.2.3 Emulsifying activity and emulsion stability index of SPC–carrageenan conjugates.** The emulsifying activity index (EAI) and emulsion stability index (ESI) were analyzed using the method by Siddiqui *et al.*<sup>39</sup> with some modifications. 22.5 ml of SPC–CG conjugates (2 mg ml<sup>-1</sup>) and 7.5 ml of red palm oil were homogenized for 5 min at 10 000 rpm using a digital homogenizer (Ultra-Turrax T50, IKA, Staufen, Germany). Then, 50 μl of emulsion was taken and added to 5 ml of 0.1% SDS solution. The absorbance of diluted emulsion was recorded at 500 nm at 0 and 10 min intervals using a UV-Vis spectrometer (UV-1800, Shimadzu, Kyoto, Japan), with 0.1% SDS used as a blank control. The emulsifying activity index (EAI) and emulsion stability index (ESI) were calculated using equations as follows:

$$EAI (\text{m}^2/\text{g}) = \frac{2 \times 2.303 \times A_0 \times DF}{C \times L \times \theta \times 10.000} \quad (2)$$

$$ESI (\text{min}) = \frac{A_0}{A_0 - A_{10}} \times \Delta t \quad (3)$$

where DF is the dilution factor,<sup>40</sup>  $A_0$  and  $A_{10}$  are the sample's absorbance at 0 and 10 min, respectively. C is the protein

concentration (g ml<sup>-1</sup>), L is the optical path length of the cuvette (1 cm), and  $\theta$  is the oil phase fraction of the emulsion (0.25).

### 2.3 Preparation of microencapsulated red palm oil

Microencapsulation of RPO was conducted using emulsification as a pre-step to spray drying. Microcapsules were prepared in various ratios of oil to wall materials (1 : 1; 1 : 1.5 : 1 : 2; 1 : 2.5; and 1 : 3). Wall materials dissolved in deionized water at a concentration of 3% (w/w), and the mixture was stirred at 1000 rpm for 30 minutes. RPO was added to the mixture and homogenized with an Ultra-Turrax (Ultra-Turrax T50, IKA, Staufen, Germany) at 15 000 rpm for 15 minutes. The coarse emulsion solution was then homogenized at a pressure of 350 bar in the first stage and 70 bar in the second stage using a high-pressure homogenizer (GEA Lab Homogenizer PandaPLUS 2000).<sup>41</sup> Subsequently, the microcapsules were prepared using a spray dryer (BUCHI Mini Spray Dryer B-290) at an inlet temperature of 200 °C and a feed rate of 8 ml min<sup>-1</sup>. The wall materials used were conjugates SPC–CG and simple mix SPC–CG.

**2.3.1 Encapsulation efficiency.** Encapsulation efficiency (EE) is defined as the percentage of carotene encapsulated in relation to the carotene content initially added. Carotene analysis was determined using the method by Jarunglumlert *et al.*<sup>42</sup> with modifications. 0.1 g microcapsules were dispersed in 10 ml hexane and stirred for 5 min at 100 rpm to extract surface carotenoids, or at 1000 rpm for 6 hours to obtain total carotenoid content at ambient temperature. The mixture was centrifuged at 4000 rpm and 25 °C for 10 min. The absorbance of the supernatant was measured using a UV-Vis spectrometer (UV-1800, Shimadzu, Kyoto, Japan) at 450 nm. Encapsulation efficiency (EE) was determined by calculating the ratio of trapped carotene (TC-FC) to the total carotene (TC), as stated in eqn (4):

$$EE (\%) = \frac{(TC - FC)}{TC} \times 100\% \quad (4)$$

where EE is the encapsulation efficiency (%), TC is the total carotene content of microcapsules (%), and FC is the free carotene content of microcapsules (%).

**2.3.2 Moisture content.** Moisture content (MC) of microcapsules was determined by oven drying (Memmert UN260 Plus). 0.1 g samples were heated at 105 °C for 24 hours, and the percentage of moisture was determined by comparing the initial and final weights of the sample.

**2.3.3 Colour.** The color profile of the microcapsules was assessed using a Chroma Meter (Konica Minolta Chroma Meter CR-400), including  $L^*$  (lightness),  $a^*$  (redness/greenness), and  $b^*$  (yellowness/blueness) values. Meanwhile, the determination of the total color difference ( $\Delta E$ ) and calculation of the whiteness index (WI) were carried out using the following formula.

$$\Delta E = \sqrt{(\Delta L^*)^2 + (\Delta a^*)^2 + (\Delta b^*)^2} \quad (5)$$

**2.3.4 Morphological properties.** The morphological properties of microencapsulated samples were observed using



a scanning electron microscope (Model: JSM-6510LA, JEOL, Japan). Powders were attached to SEM stubs, and then the specimens were coated with gold using an Auto Fine Coater (JFC-1600). SEM images were captured at 5000 $\times$  magnification.

**2.3.5 Intestinal *in situ* absorption studies.** The *in situ* intestinal absorption was performed using the method reported by Shao *et al.*<sup>43</sup> with slight modifications. The mice were fasted for 24 hours but allowed free access to water. First, the rats were anesthetized using ketamine *via* intramuscular injection in the inner thigh of the rat. The rats remained unconscious during the experiment, and the exposed intestine was covered with gauze. The intestinal segment was washed with 0.9% sodium chloride (NaCl) solution to remove any residual feces from the rat. After the feces were cleaned, microcapsule solution with a concentration of 32 mg ml<sup>-1</sup> was inserted (total solution volume was 30 ml). The flow rate was 0.25 ml min<sup>-1</sup>. Each perfusion experiment lasted for 120 minutes, and the samples were collected at the end of the experiment. The samples were centrifuged at 4000 rpm for 10 minutes. Then, the absorbance of the supernatant was measured using a UV-Vis spectrometer (UV-1800, Shimadzu, Kyoto, Japan) at 450 nm to determine the total carotene.

#### 2.4 Preparation of dark chocolate bars

Red palm oil microcapsules were added into previously melted (at 50–55 °C) dark chocolate compounds at the following amount: 0% in control chocolate (Choc control), 8% in chocolate added with microcapsules prepared with SPC-CG conjugates (ChocCG), and 8% in chocolate prepared with a simple mix of SPC-CG (ChocSM). The mixture was then mixed manually, molded into chocolate bars, and placed on a vibrating table to remove bubbles. Each sample had a constant mass of 7 g. The 8% level was selected to meet the threshold for high carotenoid content, following the criteria for provitamin A-rich foods (1.08 mg of carotenoids/100 grams of product).

**2.4.1 Melting properties.** The melting properties of chocolate samples were studied using a Differential Scanning Calorimeter (DSC) (DSC-60 Plus, Shimadzu, Japan). The analysis was performed according to the previous method.<sup>44</sup> 5 mg of the sample was placed in a sealed aluminium pan, weighed at an ambient temperature of 20 °C, and heated to 80 °C at a heat rate of 5 °C min<sup>-1</sup>.

**2.4.2 Hardness analysis.** The hardness value of the chocolate samples was determined using a texture analyzer (Texture analyzer – TA1 – AMETEK Test). The force required to break the sample was calculated using the displacement *versus* force curve at 20 °C. The trigger force was set to 0.05 N. Hardness values (N) were expressed as the mean value of 3 replicates.

**2.4.3 Rheological properties.** Rheological measurements were performed using a rheometer (HR10) based on the method described by Saputro *et al.*<sup>45</sup> with slight modifications. The chocolate was heated at 65 °C in an oven for at least 1 h before measurement. Before measurement, the samples were pre-sheared at a shear rate of 5 s<sup>-1</sup> for 15 minutes at 40 °C to ensure uniform flow conditions. During the rheological test, shear stress was recorded while increasing the shear rate from

2 s<sup>-1</sup> to 50 s<sup>-1</sup> (ramp-up), holding at 50 s<sup>-1</sup> for 60 seconds, and then decreasing it back to 2 s<sup>-1</sup> (ramp-down). The resulting data were fitted to the Casson model to determine the Casson yield stress ( $\sigma_{CA}$ ) and Casson viscosity ( $\eta_{CA}$ ). Thixotropy was calculated based on the difference in shear stress at 5 s<sup>-1</sup> between the ramp-up and ramp-down phases.

$$\tau^{\frac{1}{2}} = k\gamma^{\frac{1}{2}} + \tau_0 \quad (6)$$

where  $\tau$  is shear stress (Pa),  $\gamma$  is the shear rate (s<sup>-1</sup>),  $\tau_0$  is the slope, and  $k$  is the intercept. Casson yield stress ( $\tau_0c$ ) (Pa) is the square of the intercept, and Casson plastic viscosity ( $\eta_{CA}$ ) (Pa s) is the square of the slope.

**2.4.4 Morphology.** The morphology of the chocolate sample was observed using a Cryo Aquilos FIB to obtain a detailed view of its microstructure under cryogenic conditions.

**2.4.5 Sensory evaluation.** Sensory evaluation of dark chocolate samples was performed with 40 untrained panellists (male and female). The panellists were 18–50 years old. All participants reported that they were not on a special diet or intolerant to any ingredient in the chocolate sample, including red palm oil. The sample was delivered as a chocolate bar and presented on serving plates with different three-letter codes. Between sample assessments, the panellists were asked to consume crackers and water to cleanse their palate. The chocolate samples were evaluated using the hedonic method. The sensory attributes were presented on 9-hedonic scales, which were: (1) dislike extremely, (2) dislike very much, (3) dislike moderately, (4) dislike slightly, (5) neither like nor dislike, (6) like slightly, (7) like moderately, (8) like very much, (9) like extremely. This method was used to evaluate the panellists' preferences for the sensory characteristics of chocolate incorporated with RPO microcapsules, including appearance, aroma, flavour, texture, mouthfeel, aftertaste, off-flavour, and overall impression.

#### 2.5 Statistical analysis

Statistical analyses were performed using one-way analysis of variance (ANOVA), appropriate for assessing the effects of a single independent variable. The analysis was conducted using SPSS software version 23 (IBM Corp., Chicago, IL, USA). Where significant differences were detected, Duncan's *post hoc* test was employed to determine pairwise group differences at a 95% confidence level ( $p < 0.05$ ). All experiments and measurements were conducted in triplicate, and data were expressed as mean values  $\pm$  standard deviation (SD).

### 3 Results and discussion

#### 3.1 SPC-carrageenan conjugate formation: effect of SPC : CG ratio

In the first stage of this experiment, efforts were made to obtain SPC-CG conjugates with good properties. The influence of SPC : CG ratio was evaluated. The SPC : CG ratio that produced the best conjugates was then used in the microencapsulation steps.



**3.1.1 Formation of Amadori products and melanoidin.** The Maillard reaction occurs between the amino groups of proteins, especially from the  $\epsilon$ -amino groups of lysine, and carbonyl groups of polysaccharides. The Maillard reaction can be divided into three stages. In the early stage of the Maillard reaction, it begins with the formation of a Schiff base from the reaction between amino groups and the carbonyl group of reducing sugar, which then rearranges into Amadori products as an early indicator of the reaction. The intermediate stage involves the degradation of Amadori products through reactions such as dehydration, sugar fragmentation, and Strecker degradation, producing various volatile compounds. And the final stage involves the formation of brown nitrogen-containing polymers known as melanoidins.<sup>18</sup> Maillard reaction products were monitored by UV absorbance at 304 nm for Amadori products and 420 nm for melanoidin.<sup>46,47</sup> The browning intensity measured at 420 nm absorbance was used to characterize the development of brown chromophores, which tracked the extent and rate of the Maillard reaction.<sup>48</sup> The absorbance of the conjugates at 304 and 420 nm, influenced by the SPC : CG ratio, is shown in Fig. 1. The ratio had a significant effect ( $p < 0.05$ ) on absorbance at both wavelengths. Increasing the protein content in the conjugates enhanced the formation of Amadori products and melanoidins due to the greater availability of amino groups for the initial Schiff base. The sample with the SPC : CG ratio of 3 : 1 had the highest protein concentration, therefore providing more amino groups in the Maillard reaction process. More reactive amino acids will enhance the rate of the Maillard reaction.<sup>49</sup> The absorbance at 304 nm was generally higher than at 420 nm, which indicated that the early stage was more dominant than the advanced stage. All samples had absorbance at 420 nm below 0.2, indicating minimal browning and suggesting effective control of the Maillard reaction during the early stages.<sup>50,51</sup> Under the reaction conditions applied in this study (pH 7, 50 °C). Amadori degradation and melanoidin formation were minimized. Neutral pH enabled controlled Maillard kinetics by allowing moderate reaction rates and preventing excessive browning. The restriction of the Maillard reaction to the early and intermediate stages contributed to improving the protein functional properties, such as EAI and ESI.<sup>38</sup> The advancement of the Maillard reaction in protein-polysaccharide conjugates is undesirable, as it can reduce protein functionality;<sup>52</sup> furthermore, progression to the final

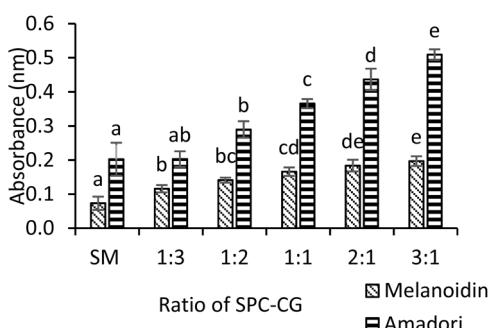


Fig. 1 The effect of SPC:CG ratio on the production of Amadori products and melanoidin.

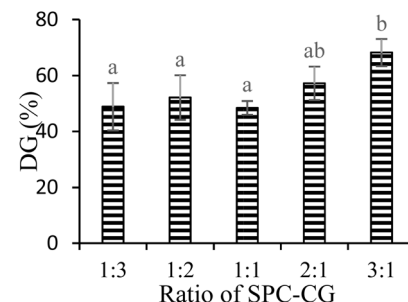


Fig. 2 The effect of SPC:CG ratio on the degree of glycation of the conjugates.

stage leads to the formation of partially insoluble products, which negatively affect emulsion stability.<sup>53</sup>

**3.1.2 Degree of glycation (DG).** Glycation of protein–polysaccharide conjugates as a strategy to improve the technical-functional characteristics of proteins provides advantages over chemical processes. The optimal result of the Maillard reaction can be seen from the reduction in free amino groups, which can be converted into the degree of glycation.<sup>54</sup> The reduction of free amino groups in SPC is related to the Maillard reaction.<sup>55</sup> Fig. 2 illustrates the DG of SPC–CG conjugates. The glycation of SPC–CG conjugates increased as the proportion of SPC increased. The 1 : 3, 1 : 2, and 1 : 1 ratios had a comparable DG. However, the DG increased significantly ( $p < 0.05$ ) when the ratio was raised to 3 : 1. These findings suggested that the DG of the Maillard reaction was influenced by the ratio of the reactants. Notably, at the SPC–CG ratio of 3 : 1, the DG peaked at 68%, while the lowest DG values were observed at the 1 : 3 ratio ( $p < 0.05$ ). This result was 3% higher than the DG obtained from the conjugation of SPI/Dextran.<sup>51</sup>

An increase in protein concentration means that more reactant groups are available in the system, which is responsible for the increase in the DG value.<sup>56</sup> This increase is due to heat, which changes the conformation of SPI, exposing more  $\epsilon$ -amino groups and promoting their reaction with aldehyde groups.<sup>57</sup> Furthermore, the higher concentration of polysaccharides increases viscosity, reducing the collision rate between protein and polysaccharide molecules and resulting in lower glycation.<sup>58</sup> The same pattern has been observed by Yao *et al.*,<sup>54</sup> who reported that a lower glycation rate was associated with an increase in the viscosity of the system. The Maillard reaction was limited to the early and intermediate stages, as shown in Fig. 1, contributing to an increased degree of glycation and was expected to improve the functionality of the conjugates.

### 3.1.3 Emulsifying activity and emulsion stability index.

Emulsifying properties are commonly reported as the emulsifying activity index (EAI) and emulsion stability index (ESI). In several studies, the most prominent characteristic of protein–polysaccharide conjugates through the Maillard reaction is their enhanced emulsifying properties.<sup>59</sup> In this study, the EAI and ESI of SPC–CG conjugates were evaluated. According to the result, the ratio of SPC–CG through the Maillard reaction had a significant effect ( $p < 0.05$ ) on EAI and ESI (Fig. 3a and b). The EAI and ESI of the SPC–CG conjugates were increased as the



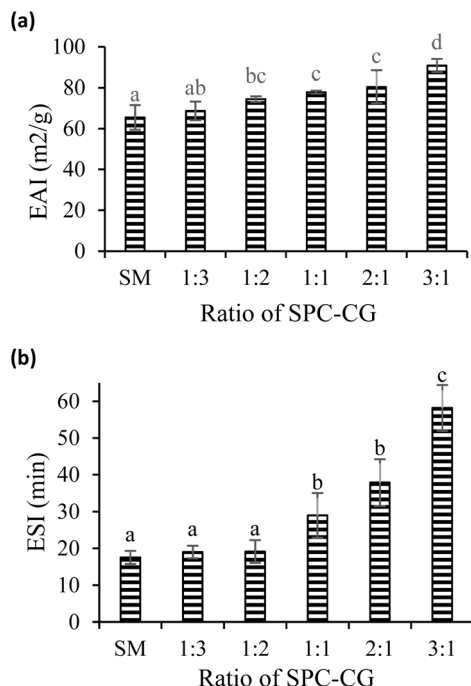


Fig. 3 The effect of SPC : CG ratio on the emulsifying activity index (a) and emulsion stability index (b) of the conjugates.

proportion of SPC added to the polysaccharide increased. The highest EAI and ESI value was  $90.82 \pm 3.23 \text{ m}^2 \text{ g}^{-1}$  and  $58.21 \pm 6.23$ , respectively, at an SPC-CG ratio of 3 : 1. Based on the results, the findings of the current study were in agreement with the results of Kusumastuti *et al.*,<sup>36</sup> who observed that the higher protein concentrations resulted in increased EAI and ESI values.

Higher EAI and ESI values indicate that the conjugate has the ability to create oil droplets of the smallest size, and the ESI value indicates the ability of the protein to produce a stable emulsion. This stability is attributed to the role of proteins in emulsion systems, where they form a cohesive viscoelastic layer at the oil-water interface.<sup>60,61</sup> Polysaccharides contribute to improving the stability of emulsions through steric repulsion.<sup>62</sup> In addition, proteins can quickly adsorb to the oil/water interface and form a protective film that prevents oil droplet aggregation and enhances emulsifying properties.<sup>63</sup> These combined interfacial and stabilizing properties make such conjugates ideal as wall materials in encapsulation, ensuring structural integrity and protection of the encapsulated core during processing and storage. The degree of glycation affects the EAI. Glycation resulted in changes of the protein secondary structure and caused the protein to be unfolded, facilitating rapid absorption at the oil-water interface. A similar trend was observed for the ESI.<sup>64</sup> The rapid adsorption of proteins at the oil-water interface leads to a significant reduction in interfacial tension.<sup>65</sup> The trend observed in the EAI and ESI aligned with the trend for Amadori products and DG. In the SPC:CG ratio range studied, higher formation of Amadori products and limited formation of melanoidin led to higher glycation (DG), resulting in improved EAI and ESI. As DG increases, more hydroxyl groups of polysaccharides are attached to the protein,

enhancing its ability to reduce surface tension at the water-oil interface, thereby producing a more stable emulsion.<sup>57</sup>

The emulsifying properties of soy protein were significantly improved after conjugation treatment.<sup>30,66</sup> For comparison, the EAI and ESI of SPC-CG conjugates (ratio 3 : 1) were compared to those of a simple mix of SPC-CG at the same ratio (Fig. 3a and b). A significant enhancement in the emulsifying properties of SPC-CG conjugates was observed as compared to the simple mix of SPC-CG. Conjugation could improve the EAI by 1.6 times and the ESI by 3.2 times. The EAI and ESI values of the SPC-CG conjugate were higher than those of the SPC-CG mixture, indicating that modification *via* the Maillard reaction effectively enhanced the emulsifying properties. This improvement is attributed to the formation of covalent bonds between protein and polysaccharide through the Maillard reaction, which increases steric repulsion and leads to the formation of a stabilizing layer around oil droplets, thereby improving emulsion stability.<sup>56</sup> Similar results were also observed, where the EAI and ESI values of SPI/MP conjugates were significantly higher than those of the SPI/MP mixture.<sup>60</sup>

### 3.2 Microencapsulation of RPO: effect of oil-to-wall material ratio

**3.2.1 The efficiency encapsulation (EE).** The oil:wall material ratio plays a fundamental role in the encapsulation efficiency.<sup>67</sup> The EE significantly increased as the proportion of the wall materials increased ( $p < 0.05$ ). The highest EE was obtained at a ratio of 1 : 3 (82.27%). The increase was associated with better oil entrapment at higher wall material concentration. This could also be due to the reduction in the time required to form a semi-permeable crust at the droplet-air interface during spray drying, making it more difficult for the oil to diffuse to the particle surface during the drying process.<sup>68</sup> In addition, rapid crust formation contributes to maintaining the integrity of the particle structure and reducing cracking, thereby enhancing oil retention.<sup>69</sup> Di Giorgio *et al.*<sup>70</sup> also reported an increase in encapsulation efficiency (EE) with higher concentrations of soy protein, achieving the highest EE of 88% at a protein-to-core ratio of 1 : 4 when prepared using a Ultra-Turrax combined with ultrasound. The lowest efficiency value of  $31.17 \pm 6.05\%$  observed at a ratio of 1 : 1 indicated that the wall material concentration was insufficient to fully cover the oil-water interface of the emulsion. This resulted in the presence of free  $\beta$ -carotene on the surface of the microcapsules. The exposure of this free  $\beta$ -carotene to the environment potentially triggers  $\beta$ -carotene degradation.<sup>71</sup> A higher oil-to-protein ratio leads to non-uniform droplet distribution, promoting creaming phenomena and consequently lower emulsion stability.<sup>68</sup>

Based on the results, microencapsulation performed at an oil:wall material (conjugates) ratio of 1 : 3 was the best one. When compared to the microcapsules prepared with wall materials from a simple mixture of SPC-CG (SPC:CG ratio 3 : 1), the conjugate wall material was still superior in terms of EE. The SM wall material could only provide an EE of 57%. This result indicated that conjugate wall materials were more effective in encapsulating RPO during the microencapsulation



Table 1 Effect of different oil-to-wall material ratios on the EE, color characteristics, and moisture content of microcapsules<sup>a</sup>

Wall materials	Ratio	EE (%)	L	a*	b*	Moisture content (%)
SPC-CG conjugates	1 : 1	31.17 ± 6.05 <sup>a</sup>	70.73 ± 1.48 <sup>a</sup>	4.00 ± 0.90 <sup>b</sup>	27.92 ± 1.96 <sup>b</sup>	3.74 ± 0.78 <sup>a</sup>
	1 : 1.5	44.82 ± 9.32 <sup>b</sup>	74.53 ± 4.08 <sup>ab</sup>	5.40 ± 1.11 <sup>bc</sup>	25.67 ± 2.19 <sup>bc</sup>	5.55 ± 1.01 <sup>bc</sup>
	1 : 2	49.36 ± 7.84 <sup>bc</sup>	70.16 ± 2.22 <sup>a</sup>	4.73 ± 1.05 <sup>b</sup>	24.48 ± 0.46 <sup>b</sup>	5.11 ± 0.26 <sup>b</sup>
	1 : 2.5	64.65 ± 5.55 <sup>d</sup>	71.25 ± 1.17 <sup>a</sup>	7.08 ± 1.57 <sup>cd</sup>	21.23 ± 0.56 <sup>a</sup>	6.77 ± 0.25 <sup>c</sup>
	1 : 3	82.27 ± 2.82 <sup>e</sup>	71.38 ± 0.50 <sup>a</sup>	8.04 ± 0.58 <sup>d</sup>	20.74 ± 0.39 <sup>a</sup>	6.80 ± 0.66 <sup>c</sup>
SPC-CG simple mixed (SM)	1 : 3	57.15 ± 2.70 <sup>cd</sup>	77.81 ± 3.43 <sup>b</sup>	-0.556 ± 0.453 <sup>a</sup>	24.45 ± 1.01 <sup>b</sup>	5.94 ± 0.62 <sup>bc</sup>

<sup>a</sup> Results having different letters in one column are significantly different ( $p < 0.05$ ).

process, likely due to the formation of a more stable layer compared to the simple mixture wall materials around the core materials.<sup>72</sup> The higher EE value might also be attributed to the conformational changes in the protein caused by heat treatment during conjugation, which exposed internal protein groups that subsequently interacted more effectively with carotene from RPO.<sup>73</sup> In the encapsulation of oily substances, the excellent emulsifying properties helped induce high encapsulation efficiency of microcapsules.<sup>74</sup> The hydrophobic part of the conjugate could bind RPO, and the hydrophilic part contributed to the stabilization through intermolecular electrostatic and steric repulsion.<sup>75</sup> Thus, rapid adsorption at the oil–water interface and high emulsifying properties led to high encapsulation efficiency and oil retention. In contrast, slow adsorption at the oil interface and poor emulsifying properties resulted in low encapsulation efficiency. It is worth noting that even microcapsules prepared with SPC-CG conjugates at a ratio of 1 : 2.5 had better EE than those prepared with SM SPC-CG at a ratio of 1 : 3, further highlighting the superiority of conjugates (Table 1).

**3.2.2 Moisture content.** In general, increasing the concentration of wall materials resulted in higher moisture content. This was reflected in the results, where the moisture content at the 1 : 1 oil-to-wall material ratio was the lowest. However, increasing the proportion of conjugate wall materials from a ratio of 1 : 1.5 to 1 : 3 only slightly increased the moisture content (Table 1). The presence of more wall materials provided more hydrophilic groups, which could bind water molecules, increasing water retention.<sup>76</sup> The presence of more oil and fewer wall materials reduced water activity caused by the decreased available space for water molecules to be absorbed and retained within the microcapsule matrix.<sup>72</sup> A similar trend was observed in the study of Lia *et al.*,<sup>30</sup> which reported that an increase in oleoresin content reduced water activity. Powder with a moisture content below 5% is still considered safe for long-term storage.<sup>77</sup> However, this moisture content level might alter the properties of the chocolate bar. Compared to the microcapsules prepared with SM wall materials, the moisture content of the microcapsules was comparable ( $p > 0.05$ ).

**3.2.3 Color properties.** The microcapsule powders exhibited a light yellow color. Color parameters lightness ( $L^*$ ), redness ( $a^*$ ), and yellowness ( $b^*$ ) of the microcapsules as a function of oil : wall material ratio are presented in Table 1. The oil : wall material ratio did not significantly ( $p > 0.05$ ) impact the  $L^*$  value of the microcapsules prepared with conjugates as the wall

materials. However, as the proportion of the wall material (conjugates) increased, the redness value ( $a^*$ ) increased. In contrast, the yellowness value ( $b^*$ ) decreased as the proportion of wall materials (conjugates) increased.

**3.2.4 Morphological properties of encapsulated red palm oil.** Morphological characteristics of the microcapsules are presented in Fig. 4. RPO microcapsule powder exhibited irregular and spherical particles. In addition, the resulting structure was round with indentations on its surface. These indentations occurred during the initial drying process, where the liquid droplets evaporated quickly.<sup>14</sup> There was a difference in the number of smaller spheres attached to the larger spheres at each applied ratio. As the wall material ratio increased, the number of smaller spheres attached to the larger spheres also increased. At an oil-to-conjugate wall material ratio of 1 : 3 (Fig. 4e), the number of smaller spheres was higher compared to the 1 : 1 ratio, which might be attributed to differences in viscosity. High viscosity tended to result in larger oil droplet sizes due to reduced shear efficiency during emulsification.<sup>78</sup> The results are similar to the study of Z. Wang *et al.*,<sup>79</sup> which showed that samples with a high percentage of CMC as the wall material tended to adhere between microcapsules.

Better microencapsulation performance observed at the 1 : 3 ratio was attributed to the higher total solid content prior to spray drying, thereby providing better protection of the core material from degradation during the drying process.<sup>10</sup> In a sample with an oil : SM wall material ratio of 1 : 3 (Fig. 4f), most of the microcapsules had larger dents on their surfaces compared to samples prepared at an oil : conjugate wall material ratio of 1 : 3. The latter had a smoother and more even surface. Particles with a rough surface, which show significant indentations, have a larger contact area compared to smooth surfaces, making the microcapsules more susceptible to degradation reactions, such as oxidation.<sup>80</sup>

**3.2.5 In situ intestinal absorption.** The experiment was conducted using the open-loop intestinal perfusion technique by measuring the carotene concentration of the solution at the beginning and end of the experiment.<sup>81</sup> The small intestine is the primary organ for digestion and nutrient absorption, including the bioactivity and absorption of carotene.<sup>82</sup> In this study, the absorption of carotene from RPO (red palm oil) encapsulated with SPC-CG conjugates in the small intestine was 82%. The initial concentration of carotene in the solution was  $249.71 \pm 3.15$  ppm, while the amount of unabsorbed carotene was  $43.95 \pm 1.65$  ppm. This value was similar to

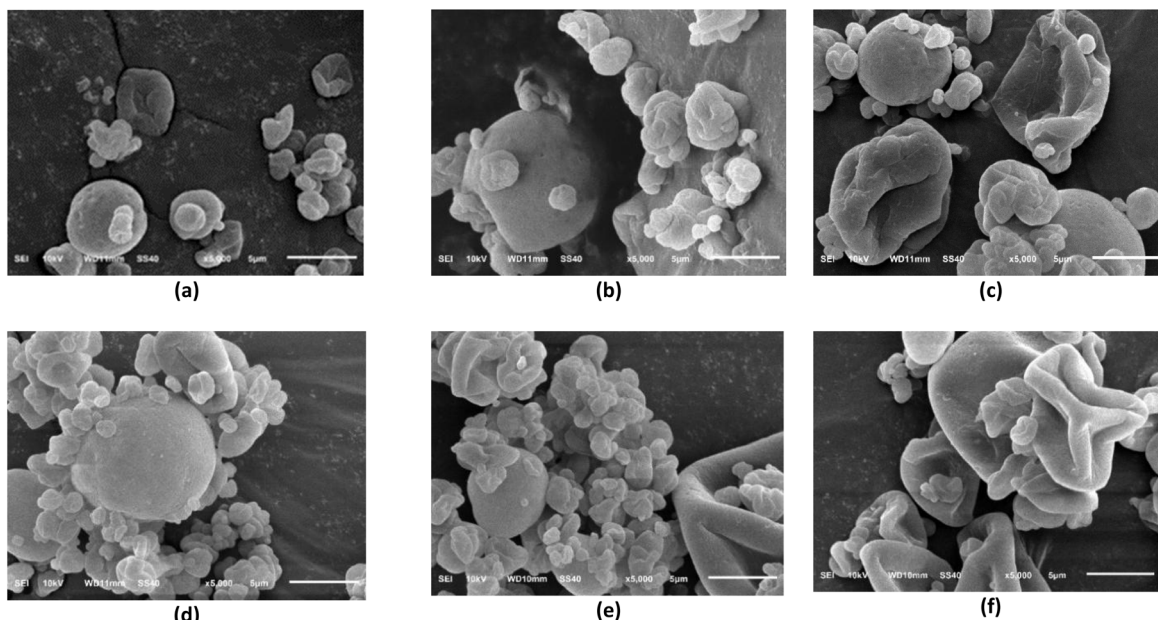


Fig. 4 SEM images of Red Palm Oil (RPO) microcapsules at different oil-to-wall material ratios: (a) 1 : 1, (b) 1 : 1.5, (c) 1 : 2, (d) 1 : 2.5, (e) 1 : 3, and (f) simple mixing (SM), observed at 5000 $\times$  magnification.

findings reporting a total  $\beta$ -carotene release of 84% from sacha inchi oil encapsulated using an *in vitro* method, indicating that the formulation process and a core-to-wall material ratio of 1 : 3 remain within a safe range for releasing carotene into the body.<sup>83</sup>

### 3.3 Influence of microencapsulated RPO addition on the properties of compound dark chocolates

**3.3.1 Melting properties.** The melting behavior of chocolate is an essential parameter for assessing its quality, particularly in relation to mouthfeel and thermal stability.<sup>84</sup> The onset melting temperature ( $T_{\text{onset}}$ ) marks the point at which specific fat crystals begin to melt, while the peak melting temperature ( $T_{\text{peak}}$ ) indicates the highest melting rate. The end melting temperature ( $T_{\text{end}}$ ) signifies the completion of the melting process. Based on the statistical analysis, the addition of RPO microcapsule powder (8%) did not result in a significant difference ( $p > 0.05$ ) compared to the control chocolate sample (Table 2). This indicates that crystal stability is similar across all samples.<sup>85</sup> The dark chocolate samples exhibited melting

point values of  $T_{\text{onset}}$  at 24–25 °C,  $T_{\text{peak}}$  at 27–29 °C, and  $T_{\text{end}}$  at 33–34 °C.

**3.3.2 Hardness.** Hardness, an essential quality attribute of chocolate strongly related to sensory perception, is the force required to attain a given deformation to the food sample.<sup>86</sup> The hardness values were in the range of 13–15 N (Table 2). It was found that the hardness of all chocolates was not significantly different ( $p > 0.05$ ). Similar results were found, showing no significant difference in hardness between the control chocolate and chocolate fortified with chia seed microcapsules.<sup>32</sup> The wall materials of the microcapsules can influence the structural network, depending on their type and concentration, which in turn plays a role in regulating the release of core oil and affects the textural characteristics of the final product.<sup>87</sup> It was suggested that the amount of RPO microcapsules added to the chocolates was not high enough to affect the hardness of the compound chocolates.

**3.3.3 Rheological properties.** Rheology is one of the crucial parameters for determining the flow properties of chocolate, which indicates the interaction between the constituent

Table 2 Melting and rheological properties of compound dark chocolate<sup>a</sup>

Sample	$T_{\text{onset}}$ (°C)	$T_{\text{peak}}$ (°C)	$T_{\text{end}}$ (°C)	$\Delta H$ (J g <sup>-1</sup> )	Hardness (N)	Casson yield value (Pa)	Casson viscosity (Pas)	Thixotropy
Choc control	25.10 ± 0.10 <sup>a</sup>	27.97 ± 0.26 <sup>a</sup>	34.58 ± 0.28 <sup>a</sup>	47.26 ± 0.13 <sup>a</sup>	15.13 ± 2.07 <sup>a</sup>	5.33 ± 0.69 <sup>a</sup>	0.32 ± 0.11 <sup>a</sup>	1.33 ± 0.46 <sup>a</sup>
ChocCG	25.49 ± 0.18 <sup>a</sup>	29.06 ± 0.05 <sup>a</sup>	34.47 ± 0.98 <sup>a</sup>	39.36 ± 5.28 <sup>a</sup>	13.28 ± 1.86 <sup>a</sup>	30.41 ± 5.01 <sup>b</sup>	0.62 ± 0.10 <sup>b</sup>	18.95 ± 4.40 <sup>b</sup>
ChocSM	24.77 ± 0.60 <sup>a</sup>	28.18 ± 0.77 <sup>a</sup>	33.85 ± 0.17 <sup>a</sup>	37.85 ± 5.40 <sup>a</sup>	13.87 ± 2.33 <sup>a</sup>	10.80 ± 2.51 <sup>a</sup>	0.66 ± 0.19 <sup>b</sup>	2.10 ± 0.46 <sup>a</sup>

<sup>a</sup> Results having different letters in one column are significantly different ( $p < 0.05$ ). Choc control: chocolate without microencapsulated RPO, ChocCG: chocolate added with microencapsulated RPO prepared with conjugated SPC-CG, ChocSM: chocolate added with microencapsulated RPO prepared with a simple mix of SPC-CG.



elements of chocolate.<sup>88</sup> The Casson yield stress is the force required to initiate the flow in molten chocolate,<sup>89</sup> related to the energy needed by the chocolate to start moving from a stationary state.<sup>85</sup> Based on Table 2, the Casson yield and viscosity of the ChocCG and ChocSM were higher compared to the control chocolate. Adding RPO microcapsule powder to chocolate increased the amount of chocolate solids and decreased the fat percentage, leading to increased interaction between particles due to the smaller amount of fat.<sup>90</sup> In addition, the increase in Casson yield stress values was due to a decrease in the particle size distribution<sup>91</sup> and a decrease in the number of coarse particles.<sup>92</sup> Smaller particle sizes will have a larger area covered, causing the interactions between particles to occur more strongly.<sup>93</sup>

Casson viscosity is related to the internal friction of the chocolate and its resistance to flow after movement begins.<sup>85,88</sup> The incorporation of RPO microcapsules into dark chocolate had a significant effect on the Casson viscosity ( $p < 0.05$ ). The value ranged from 0.32 Pa for control samples and approximately 0.6 Pa for samples with RPO microcapsules (Table 2). It indicated that samples with RPO microcapsules required greater force to maintain chocolate flow. The addition of microcapsule powder is associated with an increased surface area for particle interactions, leading to greater internal friction,<sup>85</sup> primarily due to a lower fat content. Free fat plays a key role in lubricating flow, which can reduce Casson viscosity.<sup>90</sup> The viscosity of molten chocolate is sensitive to the solid particle content and particle size distribution.<sup>94</sup>

Despite plastic viscosity and yield value, thixotropy is important in characterizing the rheology of dark compound chocolate. Thixotropic refers to the degree of agglomeration of samples affected by the chocolate component<sup>85</sup> and the mixing process (coaching) related to homogeneity. Homogeneous samples should not be thixotropic.<sup>89</sup> The addition of RPO microcapsule powder to the chocolate significantly ( $p < 0.05$ ) increased the thixotropic value (Table 2). The addition of RPO microcapsule particles affected the thixotropy value, which in turn influenced the flow properties of the chocolate.<sup>45</sup> ChocCG exhibited the highest thixotropy value, indicating a more aggregated structure compared to Choc control and ChocSM. Choc control, with the highest fat content, had a more fluid matrix and fewer aggregates, resulting in weaker thixotropic behavior (Table 3).<sup>95</sup>

**3.3.4 Morphology.** To investigate the morphological impact of red palm oil (RPO) microcapsule incorporation on compound

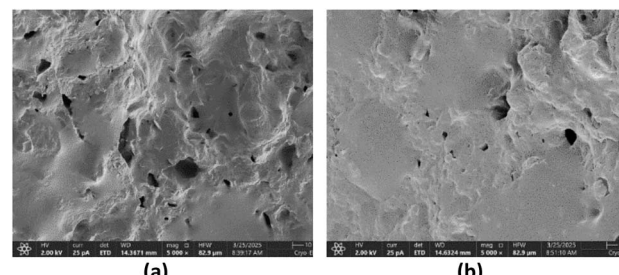


Fig. 5 Morphology of compound dark chocolate: (a) Choc control (chocolate without microencapsulated RPO) and (b) ChocCG (chocolate added with microencapsulated RPO prepared with conjugated SPC-CG).

dark chocolate, cryogenic scanning electron microscopy (cryo-SEM) was employed. The surface morphology of the control chocolate and the chocolate added with RPO microcapsules was smooth, with homogeneous structures and no apparent surface irregularities or structural defects (Fig. 5). The surface morphology and topographical characteristics of chocolate are influenced by the interactions among particles, fat, and fat-particle matrices.<sup>96</sup> Based on these observations, it can be concluded that the addition of RPO microcapsule powder remained within acceptable levels, as it did not greatly alter the surface morphology of the chocolate.

**3.3.5 Color.** The incorporation of microcapsules into the chocolate significantly ( $p > 0.05$ ) enhanced the lightness ( $L^*$ ), redness ( $a^*$ ), and yellowness ( $b^*$ ) levels. This was because the RPO microcapsule had a yellowish color, which influenced the color of the chocolate matrix, resulting in an increase in the  $L^*$ ,  $a^*$ , and  $b^*$  values. All samples exhibited positive  $a^*$  and  $b^*$  values, suggesting that all chocolates had red and yellow hues. This result was consistent with the study conducted by Hadnadev *et al.*,<sup>97</sup> which stated that the addition of fish oil microcapsules influenced the  $L^*$  value. Furthermore, the type of wall material used to encapsulate the RPO did not have effect on the color properties of the chocolate, as shown by the  $L^*$ ,  $a^*$ , and  $b^*$  values of ChocCG and ChocSM. Based on the  $\Delta E$  values obtained in this study, the color differences between ChocSM and Choc control were not easily distinguishable, as the  $\Delta E$  values were below 3. Meanwhile, ChocCG showed a noticeable colour difference compared to the control sample, with  $\Delta E$  values exceeding 3.<sup>98</sup>

Table 3 Color properties of compound dark chocolate<sup>a</sup>

Sample	$L^*$	$a^*$	$b^*$	$\Delta E$
Choc control	$24.69 \pm 0.13^a$	$2.76 \pm 0.04^a$	$2.64 \pm 0.15^a$	—
ChocCG (conjugate wall material)	$26.43 \pm 0.02^b$	$4.51 \pm 0.12^b$	$4.74 \pm 0.31^b$	$3.25 \pm 0.27^a$
ChocSM (simple mixture wall material)	$26.24 \pm 0.13^b$	$4.42 \pm 0.14^b$	$4.36 \pm 0.15^b$	$2.85 \pm 0.25^a$

<sup>a</sup> Results having different letters in one column are significantly different ( $p < 0.05$ ). Choc control: chocolate without microencapsulated RPO, ChocCG: chocolate added with microencapsulated RPO prepared with conjugated SPC-CG, ChocSM: chocolate added with microencapsulated RPO prepared with a simple mix of SPC-CG.



Table 4 Sensory evaluation<sup>a</sup>

Attributes	Hedonic test		
	Choc control	ChocCG (conjugate wall material)	ChocSM (simple mixture wall material)
Appearance	7.57 ± 1.35 <sup>a</sup>	7.60 ± 1.14 <sup>a</sup>	7.11 ± 1.30 <sup>a</sup>
Aroma	7.14 ± 1.03 <sup>a</sup>	7.48 ± 1.29 <sup>a</sup>	6.71 ± 1.48 <sup>a</sup>
Flavor	7.82 ± 0.89 <sup>ab</sup>	8.17 ± 0.82 <sup>b</sup>	7.37 ± 1.30 <sup>a</sup>
Texture	7.31 ± 1.13 <sup>a</sup>	7.62 ± 1.00 <sup>a</sup>	7.28 ± 1.34 <sup>a</sup>
Mouthfeel	7.31 ± 1.13 <sup>a</sup>	7.62 ± 1.30 <sup>a</sup>	7.28 ± 1.42 <sup>a</sup>
Aftertaste	6.91 ± 1.24 <sup>ab</sup>	7.60 ± 1.16 <sup>c</sup>	6.25 ± 1.42 <sup>a</sup>
Overall	7.74 ± 0.95 <sup>a</sup>	7.80 ± 0.90 <sup>a</sup>	7.34 ± 1.28 <sup>a</sup>

<sup>a</sup> Results having different letters in one column are significantly different ( $p < 0.05$ ). Choc control: chocolate without microencapsulated RPO, ChocCG: chocolate added with microencapsulated RPO prepared with conjugated SPC-CG, ChocSM: chocolate added with microencapsulated RPO prepared with a simple mix of SPC-CG.

**3.3.6 Sensory evaluation.** The results of the hedonic test can be found in Table 4. The results of the hedonic test provide valuable insights into consumer preferences regarding the sensory attributes of the product evaluated. RPO has a characteristic palm oil flavor, which may impact the overall taste profile of the chocolate.<sup>6</sup> Three different chocolate bars, namely: Choc control, ChocCG, and ChocSM, were presented to the panelists. The three chocolate samples had a comparable score for appearance, aroma, texture, and mouthfeel. However, panelist preferences for the flavor and aftertaste of the chocolate bar were influenced by the addition of the RPO microcapsules, with ChocCG having a higher score than ChocSM. Aftertaste refers to the sensory impression remaining in the mouth after consumption; a shorter duration of residual taste indicates a higher-quality product.<sup>99</sup>

Moreover, panelists had a higher preference for ChocCG in terms of aftertaste than the Choc control. The low preference score for flavor and aftertaste of ChocSM could be attributed to the lower ability of SPC-CG SM to mask the RPO flavor in the microcapsules than SPC-CG conjugates. No differences were found between the control chocolate and the chocolate supplemented with chia seed oil microcapsules.<sup>32</sup> This further indicates that microencapsulation with suitable wall materials could mask the unwanted flavor and aroma of the core materials. Scores above 6.0 (on a 9-point hedonic scale) represent good acceptance for dark chocolate.<sup>40</sup>

## 4 Conclusions

SPC:CG ratio influenced the EAI and ESI of the conjugates. An SPC:CG ratio of 3:1 resulted in the highest DG, leading to the highest EAI and ESI. The oil:wall material ratio affected the EE of the SPC-CG conjugates. At an oil:wall material ratio of 1:3, an EE of 82.27% was obtained. This value was even higher than that provided by SM SPC:CG wall materials. The microencapsulated RPO had an *in situ* absorption value of 82%. The incorporation of RPO microcapsules (8%) into dark chocolate bars did not significantly alter key physical properties such as melting point, hardness, morphology, and sensory characteristics. Sensory analysis showed no significant differences in the

preference score between the control chocolate and the chocolate containing RPO microcapsules (ChocCG and ChocSM). However, it significantly influenced the color properties and the flow properties, increasing both Casson yield and Casson viscosity. These findings confirm that the microencapsulation using SPC-CG conjugates as wall materials effectively masked the characteristic odor and taste of RPO, allowing its incorporation into chocolate products without compromising overall quality. It also demonstrated that microencapsulation of RPO using SPC:CG conjugates *via* the Maillard reaction is an effective strategy to enhance the physicochemical stability and sensory compatibility of RPO in functional food applications. Nevertheless, further studies are needed to evaluate the stability of the product during long-term storage and to assess the impact of RPO microcapsule addition on overall product stability and quality.

## Author contributions

Haida Setyani: investigation, formal analysis, data visualization, writing – original draft; Arima Diah Setiowati: conceptualization, methodology, data curation, validation, writing – review and editing, supervision; Sri Rahayoe: supervision, resources; Chusnul Hidayat: supervision, writing – review and editing; Arifin Dwi Saputro: methodology, validation, funding acquisition, resources.

## Conflicts of interest

There are no conflicts to declare.

## Data availability

All data generated or analyzed during this study are included in this published article and comply with research standards.

## Acknowledgements

This research was funded by the RIIM LPDP grant from the Indonesia Endowment Fund for Education Agency and



Indonesia's National Research and Innovation Agency (BRIN), according to the contract number: 34/IV/KS/06/2022 and number 2439/UN1/DITLIT/Dit-Lit/PT.01.03/2022. The first author also acknowledges the Beasiswa Unggulan scholarship provided by the Ministry of Education, Culture, Research, and Technology, which covered tuition fees during her study.

## References

- 1 A. Mancini, E. Imperlini, E. Nigro, C. Montagnese, A. Daniele, S. Orrù, *et al.*, Biological and nutritional properties of palm oil and palmitic acid: effects on health, *Molecules*, 2015, **20**(9), 17339–17361.
- 2 Z. Gao, Y. Zhu, J. Jin, Q. Jin and X. Wang, Chemical–Physical Properties of Red Palm Oils and Their Application in the Manufacture of Aerated Emulsions with Improved Whipping Capabilities, *Foods*, 2023, **12**(21), 3933.
- 3 A. W. Nur Sulihatimarsyila, H. L. N. Lau, K. M. Nabilah and I. Nur Azreena, Production of refined red palm-pressed fibre oil from physical refining pilot plant, *Case Stud. Chem. Environ. Eng.*, 2020, **2**, 100035.
- 4 O. I. Mba, M. J. Dumont and M. Ngadi, Palm oil: processing, characterization and utilization in the food industry – a review, *Food Biosci.*, 2015, **10**, 26–41.
- 5 V. H. Kurniaditya, A. D. Setiowati and C. Hidayat, Characteristics of Red Palm Oil Oleogel Based on Beeswax and Cocoa Butter and Its Application in Red Chocolate Spread, *Agritech*, 2024, **44**(4), 331–340.
- 6 A. Zeb and M. Murkovic, Determination of thermal oxidation and oxidation products of  $\beta$ -carotene in corn oil triacylglycerols, *Food Res. Int.*, 2013, **50**(2), 534–544, DOI: [10.1016/j.foodres.2011.02.039](https://doi.org/10.1016/j.foodres.2011.02.039).
- 7 S. H. Yu, M. L. Tsai, B. X. Lin, C. W. Lin and F. L. Mi, Tea catechins-cross-linked methylcellulose active films for inhibition of light irradiation and lipid peroxidation induced  $\beta$ -carotene degradation, *Food Hydrocolloids*, 2015, **44**, 491–505, DOI: [10.1016/j.foodhyd.2014.10.022](https://doi.org/10.1016/j.foodhyd.2014.10.022).
- 8 K. O. Purnama, D. Setyaningsih, E. Hambali and D. Taniwiryo, Processing, Characteristics, and Potential Application of Red Palm Oil – A review, *J. Oil Palm Res.*, 2020, **3**(2), 40–55.
- 9 D. Fu, S. Deng, D. J. McClements, L. Zhou, L. Zou, J. Yi, *et al.*, Encapsulation of  $\beta$ -carotene in wheat gluten nanoparticle-xanthan gum-stabilized Pickering emulsions: enhancement of carotenoid stability and bioaccessibility, *Food Hydrocolloids*, 2019, **89**, 80–89, DOI: [10.1016/j.foodhyd.2018.10.032](https://doi.org/10.1016/j.foodhyd.2018.10.032).
- 10 F. P. Chen, L. L. Liu and C. H. Tang, Spray-drying microencapsulation of curcumin nanocomplexes with soy protein isolate: encapsulation, water dispersion, bioaccessibility and bioactivities of curcumin, *Food Hydrocolloids*, 2020, **105**, 105821, DOI: [10.1016/j.foodhyd.2020.105821](https://doi.org/10.1016/j.foodhyd.2020.105821).
- 11 Y. Ben-Fadhel, L. Jaiswal, C. Martinez, S. Salmieri and M. Lacroix, Encapsulation, protection, and delivery of natural antimicrobials: comparison of nanoemulsion, gelled emulsion, and nanoliposomes for food application, *Food Biosci.*, 2024, **58**, 103720, DOI: [10.1016/j.fbio.2024.103720](https://doi.org/10.1016/j.fbio.2024.103720).
- 12 Y. Gao, X. Wu, D. J. McClements, C. Cheng, Y. Xie, R. Liang, *et al.*, Encapsulation of bitter peptides in water-in-oil high internal phase emulsions reduces their bitterness and improves gastrointestinal stability, *Food Chem.*, 2022, **386**, 132787, DOI: [10.1016/j.foodchem.2022.132787](https://doi.org/10.1016/j.foodchem.2022.132787).
- 13 S. He, Y. Wu, H. Wang, M. Jellicoe, D. J. Young, S. Thennadil, *et al.*, Nutrition and stability enhancement of yoghurt fortified with encapsulated algae oil through vortex fluidic device, *LWT-Food Sci. Technol.*, 2024, **191**, 115413, DOI: [10.1016/j.lwt.2023.115413](https://doi.org/10.1016/j.lwt.2023.115413).
- 14 A. A. Mohammad, F. M. Mehaya, S. H. Salem and H. M. Amer, Psyllium and okra mucilage as co-carrier wall materials for fenugreek oil encapsulation and its utilization as fat replacers in pan bread and biscuit production, *Heliyon*, 2024, **10**(3), e25321, DOI: [10.1016/j.heliyon.2024.e25321](https://doi.org/10.1016/j.heliyon.2024.e25321).
- 15 M. Al-Moghazy, H. S. El-Sayed and G. A. Abo-Elwafa, Co-encapsulation of probiotic bacteria, fish oil and pomegranate peel extract for enhanced white soft cheese, *Food Biosci.*, 2022, **50**, 102083, DOI: [10.1016/j.fbio.2022.102083](https://doi.org/10.1016/j.fbio.2022.102083).
- 16 A. Al-Hamayda, B. Abu-Jdayil, M. Ayash and J. Tannous, Advances in microencapsulation techniques using Arabic gum: a comprehensive review, *Ind. Crops Prod.*, 2023, **205**, 117556, DOI: [10.1016/j.indcrop.2023.117556](https://doi.org/10.1016/j.indcrop.2023.117556).
- 17 T. O. Hay, J. R. Nastasi, S. Prakash and M. A. Fitzgerald, Comparison of Gidyea gum, gum Arabic, and maltodextrin in the microencapsulation and colour stabilisation of anthocyanin-rich powders using freeze-drying and spray-drying techniques, *Food Hydrocolloids*, 2025, **163**, 111023, DOI: [10.1016/j.foodhyd.2024.111023](https://doi.org/10.1016/j.foodhyd.2024.111023).
- 18 A. C. M. Urango, M. A. A. Meireles and E. K. Silva, Maillard conjugates produced from proteins and prebiotic dietary fibers: technological properties, health benefits and challenges, *Trends Food Sci. Technol.*, 2024, **147**, 104438, DOI: [10.1016/j.tifs.2024.104438](https://doi.org/10.1016/j.tifs.2024.104438).
- 19 W. Wijaya, A. R. Patel, A. D. Setiowati and P. Van der Meeren, Functional colloids from proteins and polysaccharides for food applications, *Trends Food Sci. Technol.*, 2017, **68**, 56–69, DOI: [10.1016/j.tifs.2017.08.003](https://doi.org/10.1016/j.tifs.2017.08.003).
- 20 J. Feng, C. C. Berton-Carabin, V. Fogliano and K. Schroën, Maillard reaction products as functional components in oil-in-water emulsions: a review highlighting interfacial and antioxidant properties, *Trends Food Sci. Technol.*, 2022, **121**, 129–141.
- 21 N. Diftis and V. Kiosseoglou, Stability against heat-induced aggregation of emulsions prepared with a dry-heated soy protein isolate-dextran mixture, *Food Hydrocolloids*, 2006, **20**(6), 787–792.
- 22 X. Kan, G. Chen, W. Zhou and X. Zeng, Application of protein-polysaccharide Maillard conjugates as emulsifiers: source, preparation and functional properties, *Food Res. Int.*, 2021, **150**, 110740, DOI: [10.1016/j.foodres.2021.110740](https://doi.org/10.1016/j.foodres.2021.110740).
- 23 X. Li, Y. Fang, S. Al-Assaf, G. O. Phillips and F. Jiang, Complexation of bovine serum albumin and sugar beet



pectin: stabilising oil-in-water emulsions, *J. Colloid Interface Sci.*, 2012, **388**(1), 103–111, DOI: [10.1016/j.jcis.2012.08.018](https://doi.org/10.1016/j.jcis.2012.08.018).

24 X. Gu, L. J. Campbell and S. R. Euston, Effects of different oils on the properties of soy protein isolate emulsions and gels, *Food Res. Int.*, 2009, **42**(8), 925–932, DOI: [10.1016/j.foodres.2009.04.015](https://doi.org/10.1016/j.foodres.2009.04.015).

25 J. Jiang, C. Ma, X. Song, J. Zeng, L. Zhang and P. Gong, Spray drying co-encapsulation of lactic acid bacteria and lipids: a review, *Trends Food Sci. Technol.*, 2022, **129**, 134–143, DOI: [10.1016/j.tifs.2022.09.010](https://doi.org/10.1016/j.tifs.2022.09.010).

26 K. E. Preece, N. Hooshyar and N. J. Zuidam, Whole soybean protein extraction processes: a review, *Innovative Food Sci. Emerging Technol.*, 2017, **43**, 163–172, DOI: [10.1016/j.ifset.2017.07.024](https://doi.org/10.1016/j.ifset.2017.07.024).

27 Y. Dong, Z. Wei and C. Xue, Recent advances in carrageenan-based delivery systems for bioactive ingredients: a review, *Trends Food Sci. Technol.*, 2021, **112**, 348–361, DOI: [10.1016/j.tifs.2021.04.012](https://doi.org/10.1016/j.tifs.2021.04.012).

28 M. Nooshkam and M. Varidi, Maillard conjugate-based delivery systems for the encapsulation, protection, and controlled release of nutraceuticals and food bioactive ingredients: a review, *Food Hydrocolloids*, 2020, **100**, 105389, DOI: [10.1016/j.foodhyd.2019.105389](https://doi.org/10.1016/j.foodhyd.2019.105389).

29 H. Xu, L. Yang, P. Xie, Q. Zhou, Y. Chen, E. Karrar, *et al.*, Static stability of partially crystalline emulsions: impacts of carrageenan and its blends with xanthan gum and/or guar gum, *Int. J. Biol. Macromol.*, 2022, **223**, 307–315, DOI: [10.1016/j.ijbiomac.2022.10.264](https://doi.org/10.1016/j.ijbiomac.2022.10.264).

30 C. Lia, J. Wang, J. Shi, X. Huang, Q. Peng and F. Xueb, Encapsulation of tomato oleoresin using soy protein isolate-gum aracia conjugates as emulsifier and coating materials, *Food Hydrocolloids*, 2015, **45**, 301–308, DOI: [10.1016/j.foodhyd.2014.11.022](https://doi.org/10.1016/j.foodhyd.2014.11.022).

31 V. Šeregelj, L. Pezo, O. Šovljanski, S. Lević, V. Nedović, S. Markov, *et al.*, New concept of fortified yogurt formulation with encapsulated carrot waste extract, *LWT-Food Sci. Technol.*, 2021, **138**, 110732.

32 B. M. Razavizadeh and P. Tabrizi, Characterization of fortified compound milk chocolate with microencapsulated chia seed oil, *LWT-Food Sci. Technol.*, 2021, **150**, 111993, DOI: [10.1016/j.lwt.2021.111993](https://doi.org/10.1016/j.lwt.2021.111993).

33 S. T. Talawar, R. Chetana, B. S. Roopa and G. Suresh Kumar, Effect of wheat bran oil concentrates on quality and nutrition of WBO dark compound chocolates, *LWT-Food Sci. Technol.*, 2021, **142**, 111005.

34 O. Kaltsa, A. Alibade, E. Bozinou, D. P. Makris and S. I. Lalas, Encapsulation of *Moringa oleifera* Extract in Ca-Alginate Chocolate Beads: Physical and Antioxidant Properties, *J. Food Qual.*, 2021, **2021**, 5549873.

35 M. Grassia, M. C. Messia, E. Marconi, S. Demirkol, F. Erdoğdu, F. Sarghini, *et al.*, Microencapsulation of Phenolic Extracts from Cocoa Shells to Enrich Chocolate Bars, *Plant Foods Hum. Nutr.*, 2021, **76**(4), 449–457.

36 M. R. Kusumastuti, S. Yuliani, C. Hidayat and A. D. Setiowati, Modification techno-functional properties of spirulina protein concentrates (*Arthrospira Platensis*) as O/W emulsifier by conjugation and electrostatic complexations, *Innovative Food Sci. Emerging Technol.*, 2024, **95**, 103727, DOI: [10.1016/j.ifset.2024.103727](https://doi.org/10.1016/j.ifset.2024.103727).

37 I. Kutzli, J. Weiss and M. Gibis, Glycation of Plant Proteins Via Maillard Reaction : Reaction Food Application, *Foods*, 2021, **10**(376), 1–40.

38 Z. Zhang, G. Holden, B. Wang and B. Adhikari, Maillard reaction-based conjugation of Spirulina protein with maltodextrin using wet-heating route and characterisation of conjugates, *Food Chem.*, 2023, **406**, 134931, DOI: [10.1016/j.foodchem.2022.134931](https://doi.org/10.1016/j.foodchem.2022.134931).

39 M. Siddiqui, M. Ghamry, H. Golshany, C. Yang, Q. A. Al-Maqtari, W. Al-Ansi, *et al.*, Structural and functional characterization of mung bean protein-peach gum conjugate through the Maillard reaction as a novel encapsulation agent, *Prog. Org. Coat.*, 2024, **188**, 108201, DOI: [10.1016/j.porgcoat.2023.108201](https://doi.org/10.1016/j.porgcoat.2023.108201).

40 P. B. Botelho, M. Galasso, V. Dias, M. Mandrioli, L. P. Lobato, M. T. Rodriguez-Estrada, *et al.*, Oxidative stability of functional phytosterol-enriched dark chocolate, *Lwt*, 2014, **55**(2), 444–451, DOI: [10.1016/j.lwt.2013.09.002](https://doi.org/10.1016/j.lwt.2013.09.002).

41 R. G. S. Candraningrum, A. D. Setiowati and C. Hidayat, Electrostatic-Maillard formation of coconut protein Concentrate-Pectin conjugate for Oil-in-Water Emulsion: Effects of Ratio, Temperature, and pH, *J. Saudi Soc. Agric. Sci.*, 2023, **22**(1), 18–24, DOI: [10.1016/j.jssas.2022.05.004](https://doi.org/10.1016/j.jssas.2022.05.004).

42 T. Jarunglumlert, K. Nakagawa and S. Adachi, Influence of aggregate structure of casein on the encapsulation efficiency of  $\beta$ -carotene entrapped via hydrophobic interaction, *Food Struct.*, 2015, **5**, 42–50, DOI: [10.1016/j.foastr.2015.05.001](https://doi.org/10.1016/j.foastr.2015.05.001).

43 B. Shao, C. Cui, H. Ji, J. Tang, Z. Wang, H. Liu, *et al.*, Enhanced oral bioavailability of piperine by self-emulsifying drug delivery systems: in vitro, in vivo and in situ intestinal permeability studies, *Drug Delivery*, 2015, **22**(6), 740–747.

44 A. D. Saputro, D. Van de Walle, S. Kadivar, M. D. Bin Sintang, P. Van der Meeren and K. Dewettinck, Investigating the rheological, microstructural and textural properties of chocolates sweetened with palm sap-based sugar by partial replacement, *Eur. Food Res. Technol.*, 2017, **243**(10), 1729–1738.

45 A. D. Saputro, D. Van de Walle, B. A. Caiquo, M. Hinneh, M. Kluczkyoff and K. Dewettinck, Rheological behaviour and microstructural properties of dark chocolate produced by combination of a ball mill and a liquefier device as small scale chocolate production system, *LWT-Food Sci. Technol.*, 2019, **100**, 10–19.

46 Y. He and B. Vardhanabuti, Improved Heat Stability of Whey Protein Isolate by Glycation with Inulin, *Dairy*, 2021, **2**(1), 135–147.

47 F. C. De Oliveira, J. S. Dos Reis Coimbra, E. B. De Oliveira, M. Q. R. B. Rodrigues, R. C. Sabioni, B. W. S. De Souza, *et al.*, Acacia gum as modifier of thermal stability, solubility and emulsifying properties of  $\alpha$ -lactalbumin, *Carbohydr. Polym.*, 2015, **119**, 210–218, DOI: [10.1016/j.carbpol.2014.11.060](https://doi.org/10.1016/j.carbpol.2014.11.060).



48 M. Nooshkam and A. Madadlou, Microwave-assisted isomerisation of lactose to lactulose and Maillard conjugation of lactulose and lactose with whey proteins and peptides, *Food Chem.*, 2016, **200**, 1–9, DOI: [10.1016/j.foodchem.2015.12.094](https://doi.org/10.1016/j.foodchem.2015.12.094).

49 H. Cui, J. Yu, Y. Zhai, L. Feng, P. Chen, K. Hayat, *et al.*, Formation and fate of Amadori rearrangement products in Maillard reaction, *Trends Food Sci. Technol.*, 2021, **115**, 391–408, DOI: [10.1016/j.tifs.2021.06.055](https://doi.org/10.1016/j.tifs.2021.06.055).

50 Z. Zhang, W. Chen, X. Zhou, Q. Deng, X. Dong, C. Yang, *et al.*, Astaxanthin-loaded emulsion gels stabilized by Maillard reaction products of whey protein and flaxseed gum: physicochemical characterization and in vitro digestibility, *Food Res. Int.*, 2021, **144**, 110321, DOI: [10.1016/j.foodres.2021.110321](https://doi.org/10.1016/j.foodres.2021.110321).

51 F. Wang, S. Dai, J. Ye, X. Yang, J. Xu, S. Zhang, *et al.*, Soy protein isolate/dextran glycation conjugates: fabrication through ultrasound-assisted cyclic continuous reaction and their applications as carriers of anthocyanins, *Int. J. Biol. Macromol.*, 2025, **294**, 139485.

52 A. D. Setiowati, W. Wijaya and P. Van der Meeren, Whey protein-polysaccharide conjugates obtained via dry heat treatment to improve the heat stability of whey protein stabilized emulsions, *Trends Food Sci. Technol.*, 2020, **98**, 150–161, DOI: [10.1016/j.tifs.2020.02.011](https://doi.org/10.1016/j.tifs.2020.02.011).

53 G. Q. Huang, H. O. Wang, F. W. Wang, Y. L. Du and J. X. Xiao, Maillard reaction in protein-polysaccharide coacervated microcapsules and its effects on microcapsule properties, *Int. J. Biol. Macromol.*, 2020, **155**, 1194–1201, DOI: [10.1016/j.ijbiomac.2019.11.087](https://doi.org/10.1016/j.ijbiomac.2019.11.087).

54 Y. Yao, M. Zhang, Y. Yuan, B. Zhang and C. Li, Improved stability of sesame paste by peanut protein-flaxseed gum conjugation, *J. Food Eng.*, 2024, **382**, 112196, DOI: [10.1016/j.jfoodeng.2024.112196](https://doi.org/10.1016/j.jfoodeng.2024.112196).

55 A. Hussain, M. Hussain, W. Ashraf, A. Karim, S. Muhammad Aqeel, A. Khan, *et al.*, Preparation, characterization and functional evaluation of soy protein isolate-peach gum conjugates prepared by wet heating Maillard reaction, *Food Res. Int.*, 2024, **192**, 114681, DOI: [10.1016/j.foodres.2024.114681](https://doi.org/10.1016/j.foodres.2024.114681).

56 W. Chen, X. Ma, W. Wang, R. Lv, M. Guo, T. Ding, *et al.*, Preparation of modified whey protein isolate with gum acacia by ultrasound maillard reaction, *Food Hydrocolloids*, 2019, **95**, 298–307, DOI: [10.1016/j.foodhyd.2018.10.030](https://doi.org/10.1016/j.foodhyd.2018.10.030).

57 R. Li, X. Wang, J. Liu, Q. Cui, X. Wang, S. Chen, *et al.*, Relationship between Molecular Flexibility and Emulsifying Properties of Soy Protein Isolate-Glucose Conjugates, *J. Agric. Food Chem.*, 2019, **67**(14), 4089–4097.

58 C. Ma, W. Jiang, G. Chen, Q. Wang, D. J. McClements, X. Liu, *et al.*, Sonochemical effects on formation and emulsifying properties of zein-gum Arabic complexes, *Food Hydrocolloids*, 2021, **114**, 106557, DOI: [10.1016/j.foodhyd.2020.106557](https://doi.org/10.1016/j.foodhyd.2020.106557).

59 F. Kouravand, F. Shahidi, A. Koocheki and M. Fathi, Characterization and emulsifying properties of whey protein isolate-basil seed gum conjugates prepared by Maillard reaction, *J. Dispersion Sci. Technol.*, 2024, **45**(11), 2226–2239, DOI: [10.1080/01932691.2023.2263540](https://doi.org/10.1080/01932691.2023.2263540).

60 X. Ma, C. Chi, Y. Pu, S. Miao and D. Liu, Conjugation of soy protein isolate (SPI) with pectin: effects of structural modification of the grafting polysaccharide, *Food Chem.*, 2022, **387**, 132876, DOI: [10.1016/j.foodchem.2022.132876](https://doi.org/10.1016/j.foodchem.2022.132876).

61 E. F. Ribeiro, P. Morell, V. R. Nicoletti, A. Quiles and I. Hernando, Protein- and polysaccharide-based particles used for Pickering emulsion stabilisation, *Food Hydrocolloids*, 2021, **119**, 106839, DOI: [10.1016/j.foodhyd.2021.106839](https://doi.org/10.1016/j.foodhyd.2021.106839).

62 X. Kan, Y. Hu, Y. Huang, X. Fan, G. Chen, H. Ye, *et al.*, Characterization of whey protein isolate-gum Arabic Maillard conjugate and evaluation of the effects of conjugate-stabilized emulsion on microbiota of human fecal cultures, *Food Hydrocolloids*, 2023, **134**, 108060, DOI: [10.1016/j.foodhyd.2022.108060](https://doi.org/10.1016/j.foodhyd.2022.108060).

63 F. Xue, C. Li, X. Zhu, L. Wang and S. Pan, Comparative studies on the physicochemical properties of soy protein isolate-maltodextrin and soy protein isolate-gum acacia conjugate prepared through Maillard reaction, *Food Res. Int.*, 2013, **51**(2), 490–495, DOI: [10.1016/j.foodres.2013.01.012](https://doi.org/10.1016/j.foodres.2013.01.012).

64 L. Han, J. Li, Y. Jiang, K. Lu, P. Yang, L. Jiang, *et al.*, Changes in the structure and functional properties of soybean isolate protein: effects of different modification methods, *Food Chem.*, 2024, **432**, 137214, DOI: [10.1016/j.foodchem.2023.137214](https://doi.org/10.1016/j.foodchem.2023.137214).

65 H. Parhizkar, P. Taddei, D. Weziak-bialowolska, E. Mcneely, D. Spengler, J. Guillermo, *et al.*, *J. Build. Environ.*, 2023, 110984, DOI: [10.1016/j.buildenv.2023.110984](https://doi.org/10.1016/j.buildenv.2023.110984).

66 M. F. Manzoor, X. A. Zeng, M. Waseem, R. Siddique, M. R. Javed, D. K. Verma, *et al.*, Soy protein-polyphenols conjugates interaction mechanism, characterization, techno-functional and biological properties: an updated review, *Food Chem.*, 2024, **460**, 140571, DOI: [10.1016/j.foodchem.2024.140571](https://doi.org/10.1016/j.foodchem.2024.140571).

67 E. Díaz-Montes, Wall Materials for Encapsulating Bioactive Compounds via Spray-Drying: A Review, *Polymers*, 2023, **15**(12), 2659.

68 Y. Wang, W. Liu, X. D. Chen and C. Selomulya, Micro-encapsulation and stabilization of DHA containing fish oil in protein-based emulsion through mono-disperse droplet spray dryer, *J. Food Eng.*, 2016, **175**, 74–84, DOI: [10.1016/j.jfoodeng.2015.12.007](https://doi.org/10.1016/j.jfoodeng.2015.12.007).

69 T. T. Nguyen, T. V. A. Le, N. N. Dang, D. C. Nguyen, P. T. N. Nguyen, T. T. Tran, *et al.*, Microencapsulation of Essential Oils by Spray-Drying and Influencing Factors, *J. Food Qual.*, 2021, **2021**, 5525879.

70 L. Di Giorgio, P. R. Salgado and A. N. Mauri, Encapsulation of fish oil in soybean protein particles by emulsification and spray drying, *Food Hydrocolloids*, 2019, **87**, 891–901, DOI: [10.1016/j.foodhyd.2018.09.024](https://doi.org/10.1016/j.foodhyd.2018.09.024).

71 Q. Lin, H. Jiang, X. Li, D. J. McClements, S. Sang, J. Wang, A. Jiao, Z. Jin and C. Qiu, Encapsulation and protection of  $\beta$ -carotene in Pickering emulsions stabilized by chitosan-



phytic acid-cyclodextrin nanoparticles, *Food Biosci.*, 2024, **59**, 103845.

72 A. Hussain, M. Hussain, W. Ashraf, K. Ali, A. Hussain, H. M. Phylo, *et al.*, Encapsulation, optimization, and characterization of lycopene using soy protein isolate-peach gum conjugate as wall material, *Food Biosci.*, 2024, **62**, 105548, DOI: [10.1016/j.fbio.2024.105548](https://doi.org/10.1016/j.fbio.2024.105548).

73 J. Zhao, S. Xu, L. Gu, F. Yang, X. Fang and S. Gao, High internal phase emulsions gels stabilized by soy protein isolate and rutin complexes: encapsulation, interfacial properties and in vitro digestibility, *LWT-Food Sci. Technol.*, 2024, **203**, 116317, DOI: [10.1016/j.lwt.2024.116317](https://doi.org/10.1016/j.lwt.2024.116317).

74 H. R. Sharif, H. D. Goff, H. Majeed, M. Shamoon, F. Liu, J. Nsor-Atindana, *et al.*, Physicochemical properties of  $\beta$ -carotene and eugenol co-encapsulated flax seed oil powders using OSA starches as wall material, *Food Hydrocolloids*, 2017, **73**, 274–283.

75 P. G. Nagaraju, P. Sindhu, T. Dubey, S. Chinnathambi, C. G. Poornima Priyadarshini and P. J. Rao, Influence of sodium caseinate, maltodextrin, pectin and their Maillard conjugate on the stability, in vitro release, anti-oxidant property and cell viability of eugenol-olive oil nanoemulsions, *Int. J. Biol. Macromol.*, 2021, **183**, 158–170, DOI: [10.1016/j.ijbiomac.2021.04.122](https://doi.org/10.1016/j.ijbiomac.2021.04.122).

76 M. Dabestani, R. Kadkhodaei, G. O. Phillips and S. Abbasi, Persian gum: a comprehensive review on its physicochemical and functional properties, *Food Hydrocolloids*, 2018, **78**, 92–99, DOI: [10.1016/j.foodhyd.2017.06.006](https://doi.org/10.1016/j.foodhyd.2017.06.006).

77 I. Tontul and A. Topuz, Spray-drying of fruit and vegetable juices: effect of drying conditions on the product yield and physical properties, *Trends Food Sci. Technol.*, 2017, **63**, 91–102, DOI: [10.1016/j.tifs.2017.03.009](https://doi.org/10.1016/j.tifs.2017.03.009).

78 S. Drusch, Y. Serfert, M. Scampicchio, B. Schmidt-Hansberg and K. Schwarz, Impact of physicochemical characteristics on the oxidative stability of fish oil microencapsulated by spray-drying, *J. Agric. Food Chem.*, 2007, **55**(26), 11044–11051.

79 Z. Wang, X. Yu, L. Song, J. Jiao, S. Prakash and X. Dong, Encapsulation of  $\beta$ -carotene in gelatin-gum Arabic-sodium carboxymethylcellulose complex coacervates: enhancing surimi gel properties and exploring 3D printing potential, *Int. J. Biol. Macromol.*, 2024, **278**, 134129, DOI: [10.1016/j.ijbiomac.2024.134129](https://doi.org/10.1016/j.ijbiomac.2024.134129).

80 S. A. Fioramonti, E. M. Stepanic, A. M. Tibaldo, Y. L. Pavón and L. G. Santiago, Spray dried flaxseed oil powdered microcapsules obtained using milk whey proteins-alginate double layer emulsions, *Food Res. Int.*, 2019, **119**, 931–940, DOI: [10.1016/j.foodres.2018.10.079](https://doi.org/10.1016/j.foodres.2018.10.079).

81 J. Stappaerts, J. Brouwers, P. Annaert and P. Augustijns, In situ perfusion in rodents to explore intestinal drug absorption: challenges and opportunities, *Int. J. Pharm.*, 2015, **478**(2), 665–681, DOI: [10.1016/j.ijpharm.2014.11.035](https://doi.org/10.1016/j.ijpharm.2014.11.035).

82 Q. Meng, P. Long, J. Zhou, C. T. Ho, X. Zou, B. Chen, *et al.*, Improved absorption of  $\beta$ -carotene by encapsulation in an oil-in-water nanoemulsion containing tea polyphenols in the aqueous phase, *Food Res. Int.*, 2019, **116**, 731–736, DOI: [10.1016/j.foodres.2018.09.004](https://doi.org/10.1016/j.foodres.2018.09.004).

83 A. El Ghazzaqui Barbosa, A. B. T. Constantino, L. P. H. Bastos and E. E. Garcia-Rojas, Encapsulation of sacha inchi oil in complex coacervates formed by carboxymethylcellulose and lactoferrin for controlled release of  $\beta$ -carotene, *Food Hydrocolloids Health*, 2022, **2**, 100047, DOI: [10.1016/j.fhfh.2021.100047](https://doi.org/10.1016/j.fhfh.2021.100047).

84 C. Drosou and M. Krokida, Enrichment of White Chocolate with Microencapsulated  $\beta$ -Carotene: Impact on Quality Characteristics and  $\beta$ -Carotene Stability during Storage, *Foods*, 2024, **13**(17), 2699.

85 K. Y. Wong, Y. Y. Thoo, C. P. Tan and L. F. Siow, Effect of alternative sweetener and carbohydrate polymer mixtures on the physical properties, melting and crystallization behaviour of dark compound chocolate, *Food Chem.*, 2024, **431**, 137118, DOI: [10.1016/j.foodchem.2023.137118](https://doi.org/10.1016/j.foodchem.2023.137118).

86 D. R. A. Muhammad, A. D. Saputro, H. Rottiers, D. Van de Walle and K. Dewettinck, Physicochemical properties and antioxidant activities of chocolates enriched with engineered cinnamon nanoparticles, *Eur. Food Res. Technol.*, 2018, **244**(7), 1185–1202, DOI: [10.1007/s00217-018-3035-2](https://doi.org/10.1007/s00217-018-3035-2).

87 O. S. Toker, N. Konar, H. R. Pirouzian, S. Oba, D. G. Polat, İ. Palabiyik, *et al.*, Developing functional white chocolate by incorporating different forms of EPA and DHA – effects on product quality, *LWT-Food Sci. Technol.*, 2018, **87**, 177–185.

88 M. Hinneh, D. Van de Walle, J. Haeck, E. E. Abotsi, A. De Winne, A. D. Saputro, *et al.*, Applicability of the melanger for chocolate refining and Stephan mixer for conching as small-scale alternative chocolate production techniques, *J. Food Eng.*, 2019, **253**, 59–71.

89 R. P. Aidoo, N. D. Clercq, E. O. Afoakwa and K. Dewettinck, Optimisation of processing conditions and rheological properties using stephan mixer as conche in small-scale chocolate processing, *Int. J. Food Sci. Technol.*, 2014, **49**(3), 740–746.

90 E. O. Afoakwa, A. Paterson and M. Fowler, Factors influencing rheological and textural qualities in chocolate – a review, *Trends Food Sci. Technol.*, 2007, **18**(6), 290–298.

91 J. Deou, H. Bessaies-Bey, F. Declercq, P. Smith, S. Debon, J. Wallecan, *et al.*, Decrease of the amount of fat in chocolate at constant viscosity by optimizing the particle size distribution of chocolate, *Food Struct.*, 2022, **31**, 100253, DOI: [10.1016/j.foostr.2022.100253](https://doi.org/10.1016/j.foostr.2022.100253).

92 H. Rohm, B. Böhme and J. Skorka, The impact of grinding intensity on particle properties and rheology of dark chocolate, *LWT-Food Sci. Technol.*, 2018, **92**, 564–568, DOI: [10.1016/j.lwt.2018.03.006](https://doi.org/10.1016/j.lwt.2018.03.006).

93 A. D. Saputro, D. Van de Walle, R. P. Aidoo, M. A. Mensah, C. Delbaere, N. De Clercq, *et al.*, Quality attributes of dark chocolates formulated with palm sap-based sugar as nutritious and natural alternative sweetener, *Eur. Food Res. Technol.*, 2017, **243**(2), 177–191.

94 M. I. Aranguren and N. E. Marcovich, How recent approaches to improve the nutritional quality of chocolate affect processing and consumer acceptance, *Curr. Opin. Food Sci.*, 2023, **50**, 100988, DOI: [10.1016/j.cofs.2023.100988](https://doi.org/10.1016/j.cofs.2023.100988).



95 V. Glycerina, F. Balestra, M. Dalla Rosa and S. Romani, Microstructural and rheological characteristics of dark, milk and white chocolate: a comparative study, *J. Food Eng.*, 2016, **169**, 165–171, DOI: [10.1016/j.foodeng.2015.08.011](https://doi.org/10.1016/j.foodeng.2015.08.011).

96 N. Konar, I. Palabiyik, A. Karimidastjerd and O. Said Toker, Chocolate microstructure: a comprehensive review, *Food Res. Int.*, 2024, **196**, 115091, DOI: [10.1016/j.foodres.2024.115091](https://doi.org/10.1016/j.foodres.2024.115091).

97 M. Hadnađev, M. Kalić, V. Krstonošić, N. Jovanović-Lješković, T. Erceg, D. Škrobot, *et al.*, Fortification of chocolate with microencapsulated fish oil: effect of protein wall material on physicochemical properties of microcapsules and chocolate matrix, *Food Chem.:X*, 2023, **17**, 100583.

98 E. A. Ifeduba and C. C. Akoh, Microencapsulation of stearidonic acid soybean oil in complex coacervates modified for enhanced stability, *Food Hydrocolloids*, 2015, **51**, 136–145, DOI: [10.1016/j.foodhyd.2015.05.008](https://doi.org/10.1016/j.foodhyd.2015.05.008).

99 R. Indiarto, A. K. N. Situmorang, A. Harunaningtyas, H. R. Arifin, E. Subroto, E. R. N. Herawati, *et al.*, Reformulation of white chocolate with soy- and coconut-based vegetable ingredients incorporating encapsulated cinnamon extract: investigation of physicochemical, antioxidant, and sensory properties, *Int. J. Food Prop.*, 2024, **27**(1), 704–728, DOI: [10.1080/10942912.2024.2355904](https://doi.org/10.1080/10942912.2024.2355904).

